



Induced sputum metabolomic profiles and oxidative stress are associated with chronic obstructive pulmonary disease (COPD) severity: potential use for predictive, preventive, and personalized medicine

Tao Zhu¹ · Shanqun Li² · Jiajia Wang³ · Chunfang Liu² · Lei Gao² · Yuzhen Zeng² · Ruolin Mao² · Bo Cui² · Hong Ji⁴ · Zhihong Chen²

Received: 11 July 2020 / Accepted: 19 October 2020 / Published online: 4 November 2020

© The Author(s) 2020

Abstract

Chronic obstructive pulmonary disease (COPD) is a highly heterogeneous disease, and metabolomics plays a hub role in predictive, preventive, and personalized medicine (PPPM) related to COPD. This study thus aimed to reveal the role of induced sputum metabolomics in predicting COPD severity. In this pilot study, a total of 20 COPD patients were included. The induced sputum metabolites were assayed using a liquid chromatography-mass spectrometry (LC-MS/MS) system. Five oxidative stress products (myeloperoxidase (MPO), superoxide dismutase (SOD), glutathione (GSH), neutrophil elastase (NE), and 8-iso-PGF₂α) in induced sputum were measured by ELISA, and the metabolomic profiles were distinguished by principal component analysis (PCA) and orthogonal projections to latent structures discriminant analysis (OPLS-DA). The Kyoto Encyclopedia of Genes and Genomes (KEGG) was used for pathway enrichment analysis, and a significant difference in induced sputum metabolomics was observed between moderate and severe COPD. The KEGG analysis revealed that the glycerophospholipid metabolism pathway was downregulated in severe COPD. Due to the critical role of glycerophospholipid metabolism in oxidative stress, significant negative correlations were discovered between glycerophospholipid metabolites and three oxidative stress products (SOD, MPO, and 8-iso-PGF₂α). The diagnostic values of SOD, MPO, and 8-iso-PGF₂α in induced sputum were found to exhibit high sensitivities and specificities in the prediction of COPD severity. Collectively, this study provides the first identification of the association between induced sputum metabolomic profiles and COPD severity, indicating the potential value of metabolomics in PPPM for COPD management. The study also reveals the correlation between glycerophospholipid metabolites and oxidative stress products and their value for predicting COPD severity.

Tao Zhu and Shanqun Li contributed equally to this work.

Supplementary Information The online version contains supplementary material available at <https://doi.org/10.1007/s13167-020-00227-w>.

✉ Hong Ji
hgji@ucdavis.edu

✉ Zhihong Chen
chen.zhihong@zs-hospital.sh.cn

Tao Zhu
zhutao063020@163.com

Shanqun Li
li.shanqun@zs-hospital.sh.cn

Jiajia Wang
120202031@qq.com

Chunfang Liu
prettybear590@126.com

Lei Gao
zsgaolei@163.com

Yuzhen Zeng
vickyzyz0618@163.com

Ruolin Mao
maoruolin68@163.com

Bo Cui
1009267879@qq.com

Extended author information available on the last page of the article

Keywords Induced sputum · Chronic obstructive pulmonary disease (COPD) · Lung function · Metabolomics · Glycerophospholipid metabolism pathway · Predictive preventive personalized medicine (PPPM)

Introduction

Chronic obstructive pulmonary disease (COPD), the most common pulmonary disease worldwide, is characterized by persistent airflow limitation and incompletely reversible airway construction. The global prevalence of COPD was approximately 11.7% (95% CI 8.4%–15.0%) in 2010 [1, 2], and it has been estimated that COPD leads to more than 3 million deaths each year [1–3]. COPD is considered a highly heterogeneous disease with multiple phenotypes and endotypes [2, 4]. According to the Global Initiative for Chronic Obstructive Lung Disease (GOLD), the combination of the current severity of symptoms and a history of acute exacerbations within the previous year is recommended for assessing the phenotypes, which are divided into four different groups (A, B, C, and D), and for guiding the management of patients with COPD [2]. Moreover, the assessment of different aspects of COPD has identified a number of biomarkers [5]. For instance, the eosinophil percentage in the blood is a good biomarker for predicting the response to inhaled corticosteroids and the risk of readmission [6–8]. Nevertheless, substantial heterogeneities in clinical features, the treatment response, and prognosis have also been observed in a certain subgroup of patients with COPD [9–11]. Thus, there is an urgent need to move the management of COPD from the current “one-size-fits-all” approach to predictive, preventive, and personalized medicine (PPPM).

An imbalance in metabolic homeostasis is essential for the pathogenesis and progression of many diseases, such as cancers, diabetes, suboptimal health status (SHS), and COPD [12–21]. Mounting evidence supports the notion that metabolomics plays a hub role in the PPPM approach for different aspects of COPD [11, 12, 21–23]. Moreover, recent studies have shown that differential metabolomic profiles are associated with the COPD status in both patients and animals [22, 24–26]. Cruickshank-Quinn et al. reported that 2999 differential metabolites in plasma are associated with COPD outcomes, including the lung function, exacerbation frequency, degree of emphysema, and bronchodilator response (BDR) [22]. Pinto-Plata V et al. identified 79 differential plasma metabolites between surviving and nonsurviving COPD patients [25], and Fang W et al. found that 32 differential metabolites in plasma are associated with the COPD status in rats [26]. Therefore, a comprehensive understanding of metabolomic profiles might provide insights for the PPPM strategy for COPD.

Induced sputum is a commonly used method for differentiating the phenotypes and inflammatory endotypes of COPD and asthma. Compared with plasma, induced sputum is more

relevant to pathological alterations in the lower airway with less confounders in the results. Moreover, induced sputum is less contaminated and yields more accurate results than spontaneous sputum [27, 28]. Therefore, induced sputum is considered a material for the effective and accurate assessment of airway diseases that exhibits high safety and tolerability in clinical practice. The primary aims of this study were to reveal the role of the metabolomic profiles of induced sputum in the determination of COPD severity and to explore the metabolic biomarkers in induced sputum that can predict COPD severity.

Material and methods

Study design and population

This pilot study was performed at the Respiratory Department of Zhongshan Hospital of Fudan University from January 2017 to December 2018. This study was approved by the Research Ethics Committees of Zhongshan Hospital of Fudan University (No. B2014-108) in accordance with the Declaration of Helsinki. Informed consent was obtained from all the patients by the responsible physician or an appropriately trained staff member. Standard care and treatments were provided according to the current clinical guidelines [2, 29].

Inclusion and exclusion criteria

The inclusion criterion was stable COPD with a lung function classified as Global Initiative for Chronic Obstructive Lung Disease (GOLD) stage 2 ($50\% \leq$ forced expiratory volume in 1st second % (FEV1%) $< 80\%$) or 3 ($30\% \leq$ FEV1% $< 50\%$) [2]. Additionally, FEV1 was defined as the maximum amount of air that the subject can forcibly expel during the 1st second following maximal inhalation [30]. The exclusion criteria were as follows: age < 40 years, active pulmonary tuberculosis (TB), asthma, bronchiectasis, pneumoconiosis, interstitial lung diseases (ILDs), pulmonary thromboembolism (PTE), other chronic lung diseases, systemic steroid use within the previous 4 weeks, history of malignant diseases, renal failure, and liver failure. A total of 60 patients with stable COPD at GOLD stages 2 and 3 were recruited, and 29 were excluded based on the abovementioned criteria. Furthermore, four patients were unable to complete or tolerate sputum induction. The induced sputum from seven patients was disqualified (the sputum samples from four patients had $\geq 20\%$ squamous epithelial cells, and the sputum samples from three patients had cell counts < 3500) [31]. In the end, 20 patients with qualified

induced sputum samples were included: eight patients with COPD at GOLD stage 2 (moderate) and 12 patients with COPD at GOLD stage 3 (severe) (Fig. 1).

Clinical data collection

In our study, demographic data, underlying diseases, comorbidities, modified Medical Research Council dyspnea scale (mMRC) scores, and inhalation therapy information were recorded and collected. Routine blood, erythrocyte sedimentation

rate (ESR), C-reactive protein (CRP), and lung function tests were performed on the same day. To ensure the accuracy of the diagnosis and exclude most other lung diseases, all the patients underwent a high-resolution CT (HRCT) scan (64-channel CT machines with 64 × 0.625-mm collimation, 1.00-mm slice thickness, 1.00-mm intervals, reconstruction with standard algorithm, 120 kVp, and 90 mAs) within 24 h after admission. The radiation dose of HRCT was in the safe range [32, 33]. All CT results were reviewed by one independent radiologist and one pulmonologist at the hospital.

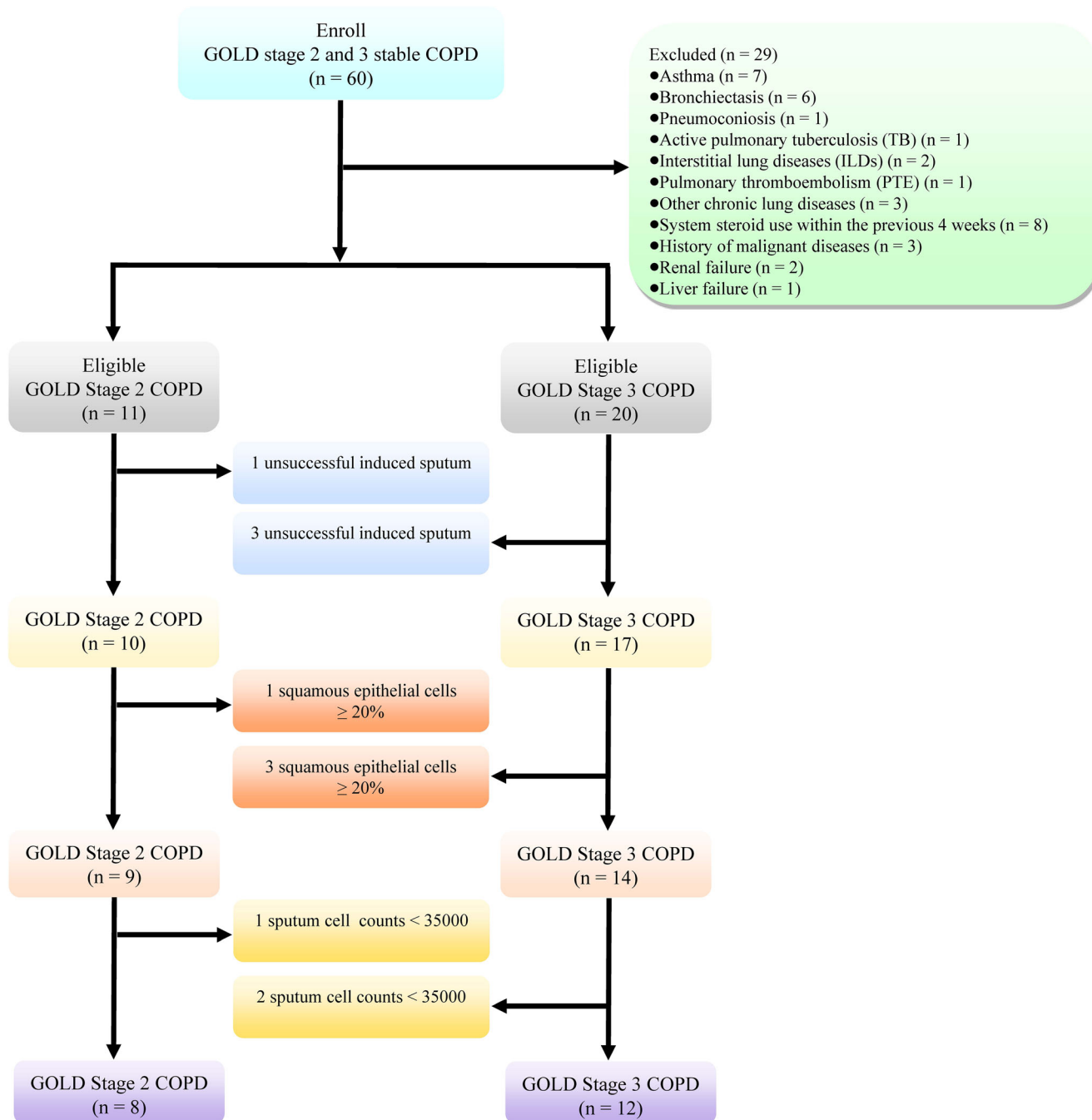


Fig. 1 Flow diagram of the study

Induced sputum collection

Prior to nebulization, the enrolled subjects drank 500 mL of water and gargled. Before hypertonic saline induction, 400 µg of salbutamol (Ventolin, GSK, UK) was inhaled. The participants were then nebulized using an ultrasonic atomizer (DeVilbiss Healthcare, Australia) with 3% NaCl for 7 min. After a short rest period, the abovementioned procedures were repeated up to three times. All phlegm clots with visibly greater solidity were carefully selected and placed in a preweighed Eppendorf tube (Eppendorf Corp. Germany). Phlegm clots less than 0.02 g indicated sputum induction failure. Phlegm clots greater than 0.02 g were processed as follows. The phlegm clots were diluted 4 times with a mixture of 0.05% dithiothreitol (Sputolysin; Calbiochem Corp., San Diego, CA, USA) and Dulbecco's PBS (ThermoFisher Corp., USA). The mixture was placed into a shaker at room temperature (RT) for 30 min until the sputum mass dissolved. The mixture of sputum and Sputolysin was passed through a nylon filter apparatus. The filtrate was collected and centrifuged at 1000 g and 4 °C for 4 min. The supernatant was collected and stored in liquid nitrogen, and the cell pellet was resuspended in PBS. Qualification of the induced sputum sample was checked by H&E staining. The samples with a squamous cell percentage ≤ 20% and/or sputum cell count > 3500 satisfied the test criteria, and the other (unqualified) samples were not subjected to further processed [31]. Subsequently, the cell sediments were resuspended in 1400 µL of quencher solution (including 200 µL of 0.085% ammonium bicarbonate (Ambic) and 1200 µL of 60% methanol). The samples were then centrifuged at 1000 g and 4 °C for 4 min, and the cell pellets and supernatants were stored in liquid nitrogen for further analyses [34].

Identification of metabolites in induced sputum

According to previous reports and the manufacturer's instructions, the metabolites of cells in induced sputum were assayed using an Q Exactive Orbitrap LC-MS/MS system [35–37]. Biotree Biotech Co., Ltd. (Shanghai, China) helped with the LC-MS analysis.

First, the cell pellet was dried under a gentle nitrogen flow, and 1000 µL of extracted solution (acetonitrile:methanol:water = 2:2:1) with 1 µg/mL internal standard was added to the sample. After vortexing for 30 s, the samples were homogenized at 35 Hz for 4 min and sonicated for 5 min in an ice-water bath. The homogenization-and-sonication cycle was repeated three times. The samples were then incubated at –20 °C for 1 h and centrifuged at 11000 rpm and 4 °C for 15 min. The resulting supernatant was transferred to a fresh glass vial for LC-MS analysis. Moreover, a mixture from various samples (10 µL) was used as a quality control (QC) sample. Subsequently, a 1290 Infinity series UHPLC System (Agilent Technologies, CA, USA)

coupled with a UPLC Waters ACQUITY UPLC HSS T3 (2.1 mm × 100 mm, 1.8 µm) and an Q exactive mass spectrometer (Thermo) was used to identify and analyze the metabolites in induced sputum. Mobile phase A consisted of 0.1% formic acid in water in the positive mode and 5 mmol/L ammonium acetate in water in the negative mode, and mobile phase B was acetonitrile. The elution gradient was set as follows: 0–1.0 min, 1% B; 1.0–8.0 min, 1–99% B; 8.0–10.0 min, 99% B; 10.0–10.1 min, 99–1% B; and 10.1–12 min, 1% B. The flow rate was 0.5 mL/min, and the injected volume was 2 µL. The QE mass spectrometer was used for its ability to acquire MS/MS spectra in the data-dependent acquisition (DDA) mode, and this process was controlled by the acquisition software (Xcalibur 4.0.27, Thermo). In this mode, the acquisition software continuously evaluates the full-scan MS spectrum. The ESI source conditions were set as follows: sheath gas flow rate of 45 Arb, Aux gas flow rate of 15 Arb, capillary temperature of 400 °C, full MS resolution of 70,000, MS/MS resolution of 17,500, collision energy of 20/40/60 eV in the normalized collisional energy (NCE) mode, and spray voltage of 4.0 kV (positive) or –3.6 kV (negative). The injection volume was 1 µL. The MS/MS spectra were measured with the Triple TOF mass spectrometer on a data-dependent acquisition (DDA) in the LC-MS experiment. Meanwhile, top 3 intensive ions (peaks) in each MS1 scan were selected for MS/MS analysis.

Levels of myeloperoxidase, superoxide dismutase, glutathione, neutrophil elastase, and 8-iso-PGF2α in induced sputum

According to our previous studies [38–41] and the manufacturer's instructions, the levels of myeloperoxidase (MPO), superoxide dismutase (SOD), glutathione (GSH), neutrophil elastase (NE), and 8-iso-PGF2α in the supernatant of induced sputum were measured by ELISA (R&D Systems, Minneapolis, MN, USA). In brief, a 96-well microplate was coated with 100 µL of the capture antibodies (MPO, SOD, GSH, NE, or 8-iso-PGF2α) overnight at 4 °C. Unbound capture antibody was blocked at RT for 1 h, and 100 µL of induced sputum supernatant was added to each well of the microplate for incubation at RT for 2 h. The detection antibody was added, and the plate was incubated at RT for 2 h. Between each step, the plate was washed with a detergent solution to remove any nonspecifically bound proteins or antibodies. Subsequently, 50 µL of termination solution was added to each well, and the absorbance was read using a microplate reader at 450 nm [38].

Statistical analysis

The data were entered into a computer spreadsheet program (Microsoft Office Excel 2010) by designated staff members. All the analyses were performed using SPSS 22.0. The

baseline characteristics of the study population are described. Continuous variables are expressed as the means \pm standard deviations (SDs), and categorical data are expressed as frequencies. Non-normally distributed continuous data are presented as the medians and interquartile ranges (IQRs). The distribution of categorical groups was examined using the Kolmogorov-Smirnov test. The categorical variables were analyzed using the chi-square test, and the continuous variables were analyzed by Student's *t* test. Ordinal variables and continuous variables without a normal distribution were analyzed with the Mann-Whitney U test. The Spearman rank correlation coefficient was used for the correlation analyses. A threshold of $P < 0.05$ was considered significant.

For the metabolomics analysis, mass spectrometry (MS) raw data files were converted to mzXML format using ProteoWizard software (version 3.0.19282) and processed with R software package XCMS (version 3.2) for peak detection, extraction, alignment, and integration [35, 42, 43]. The peaks were detected, and metabolites could be identified through the interquartile range denoising method. The missing values in the raw data were filled by half of the minimum value. Additionally, the overall normalization method was used for data analysis. To make the metabolomics data reproducible, the relative standard deviation (RSD) of the peaks in the QC samples larger than 30% were filtered out. The multivariate analysis, principal component analysis (PCA), and orthogonal projections to latent structure discriminant analysis (OPLS-DA) were performed using SIMCA software (v14.1; Sartorius Stedim Data Analytics AB, Umea, Sweden). PCA was used to show the distribution of the original data. OPLS-DA was used to further observe the separation between two groups and to further understand the variables responsible for classification. The variable importance in the projection (VIP) of the first principal component obtained in the OPLS-DA analysis was obtained. The metabolites with a VIP value > 1 in the OPLS-DA analysis and a P value < 0.05 in the univariate analysis were considered significantly different. Moreover, the OPLS-DA model quality was evaluated with standard parameters (R^2Y and Q^2) by 200 permutations. Additionally, the data were matched using BiotreeDB (V2.1) to establish a secondary mass spectrometry database for material annotation [44]. The commercial database KEGG (<http://www.genome.jp/kegg/>) was used for pathway analysis.

Results

Demographic characteristics and laboratory parameters of patients with COPD

A total of 60 patients were initially enrolled in this study, and in the end, eight patients with moderate (GOLD stage 2) COPD and 12 patients with severe (GOLD stage 3) COPD

from whom qualified induced sputum samples were obtained were included in this study (Fig. 1). The FEV1% and FEV1/FVC% values of the patients with severe COPD were noticeably lower than those of the patients with moderate COPD (Table 1). No differences in age, sex, smoking status, BMI, mMRC scores, inhalation therapies, underlying diseases, or laboratory parameters were found between the patients with moderate COPD and those with severe COPD.

Identification and quantification of LC-MS/MS system compounds

The ionization source for the LC-MS/MS was electrospray ionization, including the positive (POS) and negative (NEG) ion modes, and a total of 10,503 POS peaks and 4958 NEG peaks were found after data preprocessing (Supplementary Table S1).

Multivariate analysis of metabolites

Multivariate analyses, namely, PCA and OPLS-DA, were performed to comprehensively compare the induced sputum metabolomic profiles between moderate and severe COPD and to reveal the degree of diversity between the two groups. Four quality control (QC) samples were included to evaluate the stability and repeatability of the system, and the QCs were clustered together and separated from the samples from the study subjects, which indicated the correctness of the PCA (Fig. 2a). The PCA score plot presented clear differences between moderate and severe COPD, and one outlier was located beyond 95% Hotelling's *T*-squared ellipse (Fig. 2b). As shown in Fig. 2b, most moderate COPD samples clustered on the left, whereas all severe COPD clustered on the right. However, three moderate COPD samples located on the right were also observed in the PCA score plots.

An OPLS-DA was performed to further compare the induced sputum metabolomic profiles between moderate and severe COPD. The OPLS-DA score plot showed significant differences in the induced sputum metabolomic profiles between the moderate and severe COPD samples (Fig. 2c). As shown in Fig. 2c, all moderate COPD samples clustered on the right, whereas all severe COPD clustered on the left, and no overlap was observed. This result indicated the existence of significant differences in the induced sputum metabolomic profiles between patients with moderate COPD and those with severe COPD. Additionally, the permutation test yielded R^2Y (cum) and Q^2 (cum) values of 0.77 and -0.58 , respectively, and these results indicated the lack of overfitting and the good predictive ability of the OPLS-DA model (Fig. 2d), which indicated the suitability of the model for subsequent optimization analyses.

Table 1 The demographic data and laboratory findings from COPD patients ($n = 20$)

	Moderate COPD ($n = 8$)	Severe COPD ($n = 12$)	Statistical values	P
Sex (male, (%))	8 (100.00%)	11 (91.67%)	0.702	0.402
Age (years)	67.5000 \pm 8.60233	67.0000 \pm 5.30866	0.162	0.873
Body mass index (BMI)	21.6350 \pm 2.41780	21.8017 \pm 3.10319	-0.128	0.900
Smoking			0.208	0.901
Non-smoking	2	2		
Ex-smoking	3	5		
Current-smoking	3	5		
mMRC scores	1.2500 \pm 0.70711	1.7500 \pm 0.86603	-1.356	0.192
Lung functions				
Forced expiratory volume in 1st second % (FEV1%)	62.2250 \pm 8.02064	40.3500 \pm 7.24061	6.345	0.000*
Forced expiratory volume in 1st second/forced vital capacity % (FEV1/FVC%)	60.6788 \pm 8.07667	47.5508 \pm 9.40506	3.227	0.005*
Underlying diseases/comorbidities				
Cor pulmonale	1	1	0.093	0.761
Pulmonary hypertension (PH)	0	1	0.702	0.402
Coronary artery disease (CAD)	2	3	0.000	1.000
Hypertension	4	5	0.135	0.714
Type 2 diabetes (T2DM)	2	3	0.000	1.000
Atrial fibrillation (Af)	0	1	0.702	0.402
Inhalation therapy			0.104	0.949
ICS/LABA	3	5		
LAMA	4	6		
ICS/LABA/LAMA	1	1		
Laboratory parameters				
White blood cells (WBC) ($\times 10^9/L$)	6.4988 \pm 2.12200	6.8625 \pm 1.41555	-0.462	0.650
Neutrophils (NS) ($\times 10^9/L$)	4.2525 \pm 1.98737	4.7558 \pm 1.20220	-0.709	0.487
Lymphocytes ($\times 10^9/L$)	1.5988 \pm 0.66398	1.4308 \pm 0.42374	0.694	0.497
Eosinophils (EOS) ($\times 10^9/L$)	0.2275 \pm 0.23236	0.1833 \pm 0.10369	0.583	0.567
Neutrophils-to-lymphocytes ratio (NLR)	3.1438 \pm 2.24662	3.5950 \pm 1.34660	-0.564	0.580
NS%	63.6275 \pm 11.04820	68.9108 \pm 6.29898	-1.367	0.189
EOS%	3.4962 \pm 3.2007	2.7450 \pm 1.61699	0.697	0.495
Lymphocytes%	26.4613 \pm 10.58444	21.0542 \pm 5.78485	1.481	0.156
C-reactive protein (CRP) (mg/mL)	8.5750 \pm 10.11163	20.0750 \pm 14.78796	-1.913	0.072
Erythrocyte sedimentation rate (ESR) (mm/first hour)	14.0000 \pm 14.10167	15.6667 \pm 17.55166	-0.224	0.825
Red blood cells (RBC) ($\times 10^{12}/L$)	4.2875 \pm 0.59122	4.5325 \pm 0.24893	-1.288	0.214
Hemoglobin (Hb) (g/L)	133.7500 \pm 15.42493	139.3333 \pm 7.31541	-1.093	0.289
Platelets (PLT) ($\times 10^9/L$)	161.0000 \pm 92.48784	204.4167 \pm 60.20036	-1.278	0.218

* P value < 0.05

Identification of significantly different metabolites and pathways associated with COPD severity

In our study, 573 positive-ion-mode (POS) metabolites with VIP values > 1 in the OPLS-DA analysis and P values < 0.05 in the univariate analysis were found between moderate and severe COPD samples (Supplementary Table S2), which indicated that these 573 POS metabolites were associated with COPD severity. Among these metabolites, 237 were mass spectrometry 1 (MS1) metabolites, 21 were mass spectrometry 2 (MS2) metabolites, and 315 were “unknown” metabolites based on the BiotreeDB database. However, no negative-ion-mode (NEG) metabolites associated with COPD severity were found.

Specifically, 42 metabolites were increased and 531 metabolites were reduced in severe COPD compared with moderate

COPD (Supplementary Table S2). These 573 POS metabolites associated with COPD severity were then summarized in a volcano plot (Fig. 3a): the 42 metabolites (red spots) increased in severe compared with moderate COPD were located on the right, and the 531 reduced metabolites (blue spots) were located on the left (Fig. 3a). In addition, 1 and 20 of the 21 MS2 metabolites was found at higher and lower levels, respectively, in severe compared with moderate COPD (Supplementary Table S2). Furthermore, a heatmap was used to classify the upregulated and downregulated MS2 metabolites in patients with severe COPD compared with those with moderate COPD (Fig. 3b).

Additionally, a KEGG pathway analysis was performed to explore the enriched metabolic pathways associated with COPD severity. The results showed that the glycerophospholipid metabolism pathway was the only

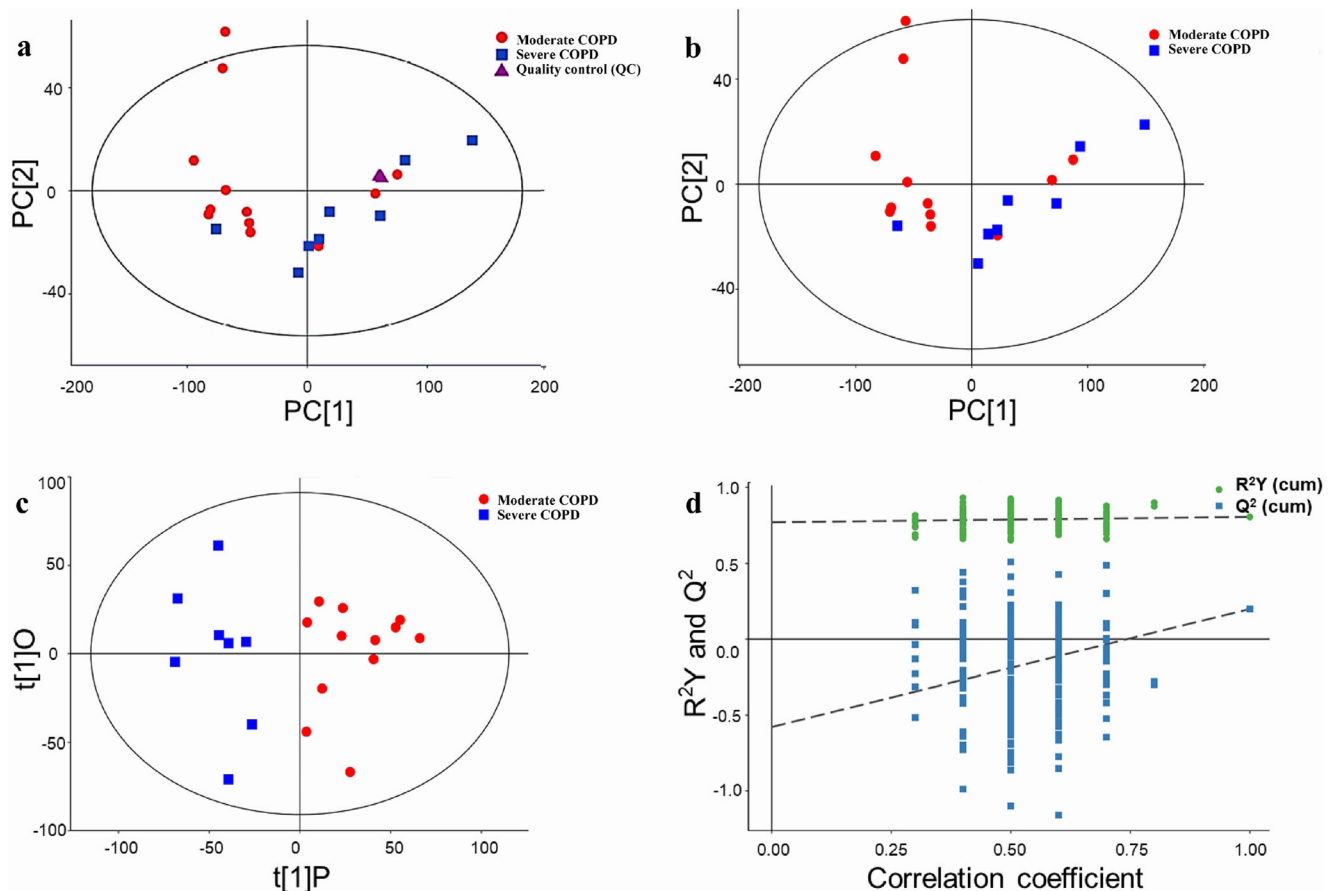


Fig. 2 PCA score plots, OPLS-DA score plot, and corresponding validation plot of OPLS-DA results derived from the metabolomics profiles of induced sputum between moderate and severe COPD. **a**

PCA score plot with four quality controls (QC). **b** PCA score plot without the QC samples. **c** OPLS-DA score plot. **d** Permutation test ($n = 200$) of the OPLS-DA model

enriched metabolic pathway associated with COPD severity, and this pathway was downregulated in severe compared with moderate COPD (Supplementary Table S2).

Predictive value of five oxidative stress products in induced sputum for predicting COPD severity

Because the glycerophospholipid metabolism pathway is essential for oxidative stress [45–47], the levels of five oxidative stress products (MPO, SOD, GSH, NE, and 8-iso-PGF2 α) in induced sputum were measured by ELISA to evaluate the association between oxidative stress and COPD severity. The levels of SOD, MPO, and 8-iso-PGF2 α in the induced sputum samples from the patients with severe COPD were significantly higher than those in the samples from the patients with moderate COPD (Table 2). No differences in GSH and NE were observed between moderate and severe COPD. Moreover, the levels of SOD (AUC = 0.885), MPO (AUC = 0.781), and 8-iso-PGF2 α (AUC = 0.813) in induced sputum showed high sensitivities and specificities for the prediction of COPD severity (Fig. 4).

Correlations between glycerophospholipids (choline, *N*-methylethanolamine phosphate, and 1-linoleoylglycerophosphocholine) and levels of oxidative stress products in induced sputum from patients with COPD

The correlations between glycerophospholipids (choline, *N*-methylethanolamine phosphate (NMethy), and 1-linoleoylglycerophosphocholine (1-LGPC)) and the levels of five oxidative stress products in induced sputum from patients with stable COPD were explored by Spearman correlation analysis. As shown in Table 3, SOD was significantly negatively correlated with three glycerophospholipids (choline, NMethy, and 1-LGPC), and 1-LGPC was markedly negatively correlated with MPO and 8-iso-PGF2 α .

Correlations between lung function and SOD, MPO, GSH, NE, and 8-iso-PGF2 α levels in induced sputum of COPD patients

Because COPD severity is defined by the degree of lung function impairments [2], the correlations between lung function (FEV1%

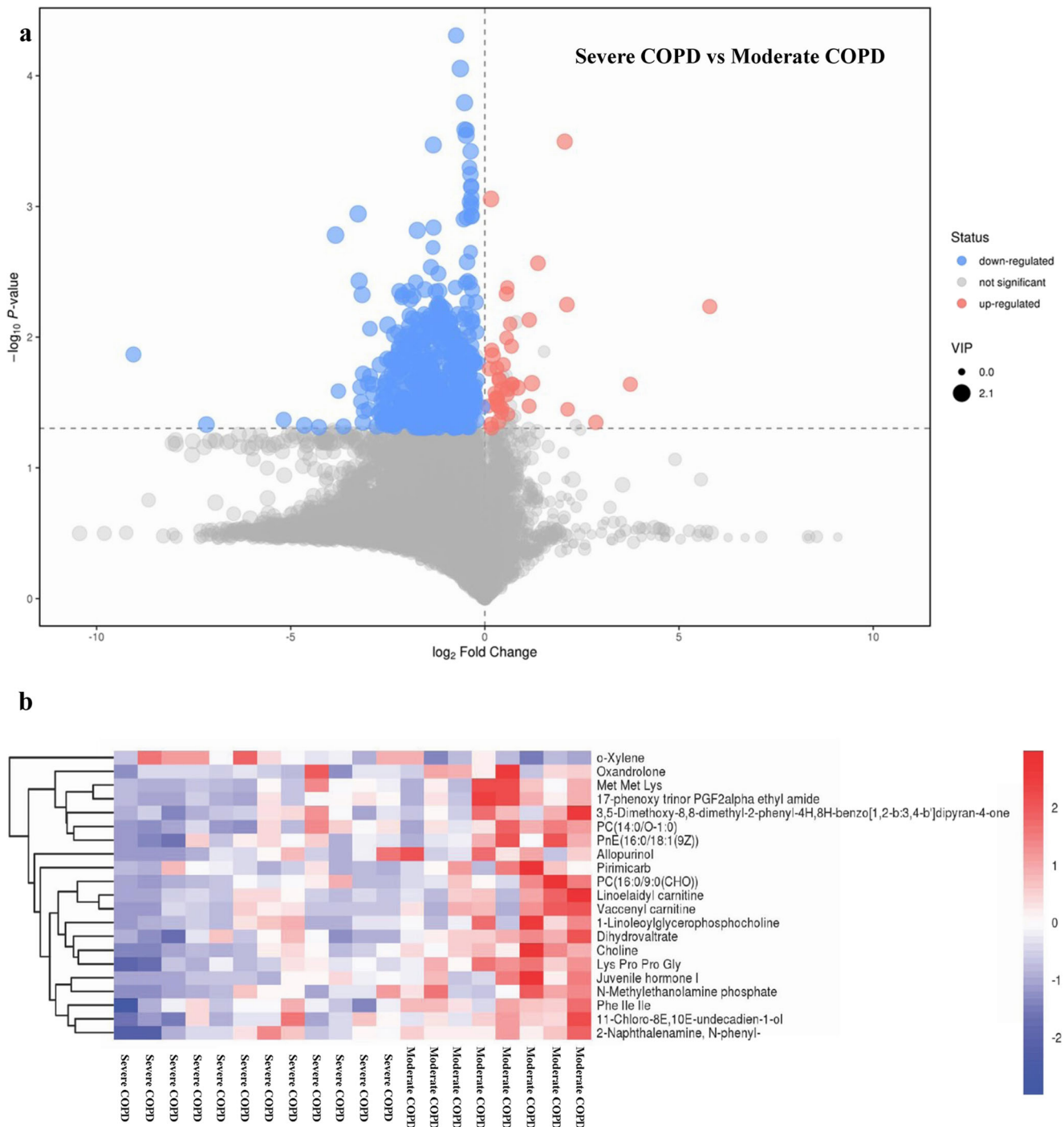


Fig. 3 Identification of the differential metabolomics profiles of induced sputum between moderate and severe COPD based on a volcano plot and hierarchical clustering analysis. **a** Volcano plot. The downregulated and upregulated metabolites in severe compared with moderate COPD are marked in blue and red, respectively. X-axis: \log_2 fold change of

metabolites; Y-axis: fold change of $-\log_{10} P$ value determined by Student's *t* test. The dot size represents the variable importance in the projection (VIP) value. **b** Heatmap of the hierarchical clustering analysis. Twenty-one MS2 differential metabolites are presented

and FEV1/FVC%) and five oxidative stress products in induced sputum from patients with stable COPD were explored by Spearman correlation analysis. Significant negative correlations were observed between FEV1% and the 8-iso-PGF2 α level and between FEV1/FVC% and the MPO and 8-iso-PGF2 α levels (Table 3).

Discussion

This pilot study provides the first demonstration of an association between the metabolomics profile of induced sputum and COPD severity, and the results indicate the potential value of induced sputum metabolomics in the PPPM-based

Table 2 The levels of SOD, MPO, GSH, NE, and 8-iso-PGF2α in induced sputum in COPD patients (n = 20)

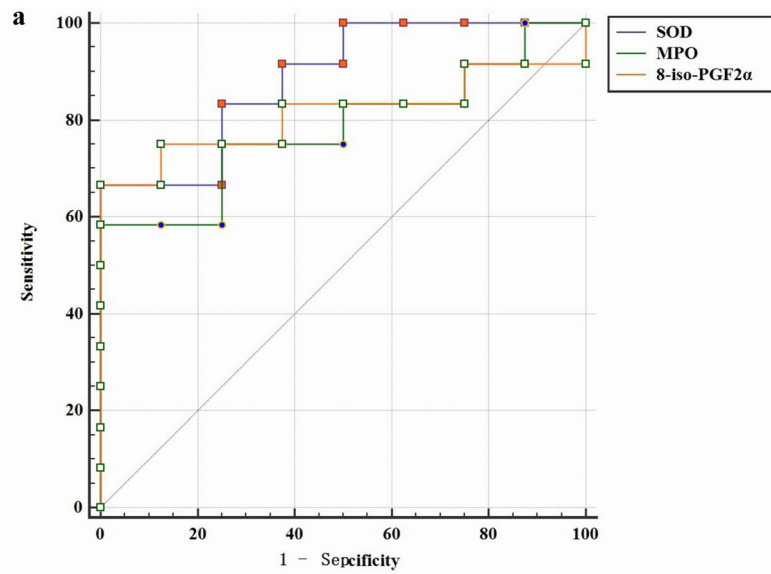
	Moderate COPD (n = 8)	Severe COPD (n = 12)	Statistical values	P
SOD (ng/mL)	2.81702750 ± 1.481169877	5.87841667 ± 1.684597522	- 4.170	0.001*
MPO (ng/mL)	5.20834875 ± 0.849961544	7.11504083 ± 2.127440318	- 2.393	0.028*
GSH (pg/mL)	48.89454875 ± 81.860376895	59.50663000 ± 100.387792570	- 0.248	0.807
NE (pg/mL)	275.44425000 ± 253.353683063	250.36500000 ± 262.347043724	0.212	0.834
8-iso-PGF2α (pmol/mL)	131.84655462 ± 50.691770294	343.47142350 ± 226.995290954	- 2.572	0.019*

*P value < 0.05

management of COPD. Simultaneously, a subset of COPD severity-associated metabolites were identified, and these were found to be promising biomarkers for predicting COPD severity. In this study, we found that 573 POS differential metabolites (DMs), including 237 MS1, 21 MS2, and 315 “unknown” metabolites, were associated with lung function impairments (GOLD stages) in patients with stable COPD. Among the 573 DMs, 42 and 531 metabolites were found at higher and lower levels, respectively, in patients with

severe COPD. Moreover, among the 21 MS2 metabolites, 1 and 20 metabolites were increased and reduced, respectively, in severe compared with moderate COPD. We then found that the glycerophospholipid metabolism pathway was associated with COPD severity. Additionally, three oxidative stress products (MPO, SOD, and 8-iso-PGF2α) in induced sputum that exhibited high sensitivities and specificities for the prediction of COPD severity were identified. We also found that the MPO and 8-iso-PGF2α levels in induced sputum were

Fig. 4 Values of the SOD, MPO, and 8-iso-PGF2α levels in induced sputum for predicting COPD severity. **a** ROC curves. **b** Sensitivity, specificity, Youden index, AUC, and cutoff value



b

The sensitivity and specificity of SOD, MPO, and 8-iso-PGF2α in induced sputum in prediction of COPD severity.

	Sensitivity	Specificity	Youden index	AUC	Cut-off value
SOD	66.67%	100%	0.6667	0.885	4.58 (ng/ml)
MPO	58.33%	100%	0.5833	0.781	6.242 (ng/ml)
8-iso-PGF2α	66.67%	100%	0.6667	0.813	227.384 (pmol/ml)

Table 3 The correlations between lung function and 3 glycerophospholipids and induced sputum 5 oxidative stress products in COPD patients ($n = 20$)

		SOD	MPO	GSH	NE	8-iso-PGF2 α
FEV1%	R	-0.405	-0.432	0.171	-0.174	-0.606
	P	0.077	0.057	0.470	0.462	0.005*
FEV1/FVC%	R	-0.313	-0.512	0.275	-0.217	-0.705
	P	0.179	0.021*	0.240	0.359	0.001*
Choline	R	-0.650	-0.409	-0.185	0.117	-0.411
	P	0.002*	0.073	0.435	0.622	0.072
NMethy	R	-0.653	-0.421	-0.188	-0.200	-0.259
	P	0.002*	0.064	0.427	0.398	0.271
1-Linoleoylglycerophosphocholine (1-LGPC)	R	-0.489	-0.514	-0.132	-0.281	-0.504
	P	0.029*	0.021*	0.578	0.230	0.024*

* P value < 0.05

negatively correlated with lung function and that the SOD, MPO, and 8-iso-PGF2 α levels in induced sputum were negatively correlated with glycerophospholipids (choline, NMethy, and 1-LGPC) in patients with stable COPD.

The prevalence of COPD has continued to increase in recent decades [2], and it has been estimated that COPD will become the third leading cause of disease-induced mortality worldwide by 2025 to 2030 [1, 2]. In addition, COPD is a highly heterogeneous disease [11]. Significant individual differences in many variables, including risk factors, clinical features, comorbidities, and therapeutic responses to prognosis, have been observed among patients with COPD [2]. From one point of view, the consideration of COPD as a single disease is less appropriate because COPD is probably a syndrome that encompasses several obstructive airway disorders that share a common exposure but differ in terms of the mechanism of the disease and the response to treatment [48, 49]. Therefore, predictive, preventive, and personalized medicine (PPPM)-based management approaches are urgently needed to guide the diagnosis, severity assessment, therapeutic options, and prognosis of COPD. Accumulating evidence obtained in recent studies reveals that abnormal metabolism plays a key role in the pathogenesis of COPD [12, 24, 50]. Compared with traditional metabolic study methods, metabolomics tools provide insight into underlying relationships among metabolites, and these findings allows researchers to obtain a complete picture of the role of metabolites in the pathogenesis of diseases. Moreover, several studies have shown that metabolomics is an ideal and promising method for evaluating the phenotype, severity, and individual differences among patients with COPD, which indicates that metabolomics is an essential tool for PPPM in COPD [12, 50]. Several studies have found distinct differences in the metabolomic profile between patients with COPD and without COPD, and similar findings have been obtained in humans and animals [24, 26, 42, 50, 51]. Fang et al. showed that 32 dysregulated metabolites in plasma are associated with the COPD status in rats

[26]. Van der Does et al. revealed that the levels of free alpha-linolenic acid, linoleic acid, eicosapentaenoic acid (EPA), omega-3, and EPA- and docosahexaenoic acid-derived oxylipins in the sputum of patients with COPD are noticeably lower than those in the sputum of healthy subjects [36]. These researchers also noticed that the levels of free arachidonic acid and docosapentaenoic acid in sputum were significantly increased in acute exacerbation of COPD (AECOPD) compared with stable COPD. Fortis et al. showed that both the serum and urine metabolomic profiles showed marked differences between patients with stable COPD and those with AECOPD [42]. Additionally, Ghosh et al. revealed that 12 differential metabolites in serum were dysregulated in patients with asthma-COPD overlap (ACO) compared with both patients with asthma and patients with COPD [51]. However, the association between the metabolomic profiles of induced sputum and COPD severity has not been previously studied. This study aimed to explore the differential metabolites in induced sputum between patients with moderate (GOLD stage 2) and severe (GOLD stage 3) stable COPD. In our study, 60 patients were enrolled, and 20 patients with qualified induced sputum samples were included: 8 with moderate (GOLD stage 2) COPD and 12 with severe (GOLD stage 3) COPD (Fig. 1). No differences in sex, age, BMI, smoking status, underlying diseases, inhalation therapies, complications, or laboratory parameters were found between these two groups. These results suggested that demographic characteristics, treatments, and included laboratory parameters are not associated with the severity of stable COPD, and these data also indicated that the internal validity of the study was good.

Induced sputum is a direct, reliable, sensitive, simple, and repeatable approach for evaluating inflammatory phenotypes and severity and for studying the pathogenesis of COPD and other pulmonary diseases, such as asthma and interstitial lung diseases (ILDs) [52–57]. In our study, the metabolites in induced sputum were assayed using a Q Exactive Orbitrap LC-

MS/MS system. The results showed that 573 POS differential metabolites were associated with COPD severity, and among these, 237 were MS1 metabolites, 21 were MS2 metabolites, and 315 were “unknown” metabolites. However, no COPD severity–associated NEG metabolites were detected. Furthermore, a KEGG pathway analysis revealed that the glycerophospholipid metabolism pathway was the only enriched metabolic pathway associated with COPD severity. Glycerophospholipids, which are the most abundant phospholipids in the lungs [58], are critical for the synthesis of pulmonary surfactant (PS), lung development, oxidative stress, lung defense, and the inflammatory response [58–60]. Xu et al. found that both the glycerophospholipids levels in both serum and the bronchoalveolar lavage fluid (BALF) are upregulated in rats with LPS-induced acute lung injury (ALI) [58]. In addition, some studies have revealed that the glycerophospholipid metabolism pathway is involved in COPD [22, 26, 61]. Telenga et al. found that the concentrations of glycerophospholipids and fatty acids in induced sputum are significantly lower in smokers with COPD than in smokers without COPD [61]. Cruickshank-Quinn et al. showed that glycerophospholipid metabolism in plasma is associated with worse airflow obstruction and more acute exacerbation in COPD [22]. Kelly et al. revealed that serum glycerophospholipids are associated with AHR, FEV1%, and FEV1/FVC% in asthmatic children, which indicates that the glycerophospholipid metabolism pathway plays a critical role in the pathogenesis of asthma [62]. Our study provides the first demonstration that glycerophospholipids in induced sputum are associated with lung function in patients with stable COPD. Therefore, the underlying mechanism of the glycerophospholipid metabolism pathway in COPD should be explored in future studies. Subsequently, multivariate analyses, namely, PCA and OPLS-DA, were used to observe the differences in the metabolomics profiles between moderate and severe COPD. Both the PCA and OPLS-DA results confirmed the significant separation between patients with moderate COPD and patients with severe COPD (Fig. 3). Collectively, these data indicate that the metabolomic profiles in induced sputum are associated with the severity of COPD.

Among the 21 MS2 metabolites (Supplementary Table S1), choline [63, 64], allopurinol [65, 66], o-xylene [67, 68], linoelaidyl carnitine [69, 70], vaccenyl carnitine [71, 72], pirimicarb [73, 74], and oxandrolone [75, 76] are involved in the oxidative stress response. It has been reported that the glycerophospholipid metabolism pathway plays an essential role in oxidative stress [22, 45–47, 77]. Therefore, the levels of five key oxidative stress products (MPO, SOD, GSH, NE, and 8-iso-PGF2 α) in induced sputum were measured by ELISA in our study. We found that the levels of SOD, MPO, and 8-iso-PGF2 α in patients with severe COPD were noticeably higher than those in patients with moderate COPD (Table 2). Moreover, negative correlations between

SOD and three glycerophospholipids (choline, NMethy, and 1-LGPC) and between 1-LGPC and MPO and 8-iso-PGF2 α were also detected (Table 3). Additionally, ROC curves were drawn to identify the values of the SOD, MPO, and 8-iso-PGF2 α levels in induced sputum for predicting COPD severity. As shown in Fig. 4, the SOD, MPO, and 8-iso-PGF2 α levels in induced sputum showed a good ability to predict the severity of stable COPD. Subsequently, we also identified significant negative correlations between FEV1% and the 8-iso-PGF2 α levels and between FEV1/FVC% and the MPO and 8-iso-PGF2 α levels (Table 3). Collectively, our results suggest that glycerophospholipid metabolism–associated oxidative stress is essential for the progression of COPD. The severity of oxidative stress is highly correlated with lung function impairments in patients with COPD. Therefore, the SOD, MPO, and 8-iso-PGF2 α levels in induced sputum are promising markers for predicting the severity of COPD in clinical practice.

Strengths and limitations

To the best of our knowledge, this study is the first to reveal that the association between the metabolomic profiles of induced sputum and COPD severity. The main strength of this study was that relatively comprehensive data, including demographic characteristics, underlying diseases, lung function, inhalation therapy, and laboratory parameters, were collected. Moreover, internal validity was good, which led to more convincing results. Of note, a chest HRCT scan was obtained from each patient, which enhanced the diagnosis accuracy and reduced the confounders. However, the limited sample size is one of the major weaknesses of this study. The roles of glycerophospholipid metabolism and its associated oxidative stress in COPD severity should be explored with a larger sample size. The predictive values of the glycerophospholipid and oxidative stress products (SOD, MPO, and 8-iso-PGF2 α) levels for COPD severity should also be replicated in other populations and ethnic groups. Additionally, the alterations in COPD severity–associated differential metabolites and oxidative stress products cannot be comprehensively evaluated by a cross-sectional design. Thus, a cohort study should be performed to further explore the mechanisms underlying the metabolomics and oxidative stress changes in the progression of COPD.

Conclusions and expert recommendations

Overall, our study provides the first identification of the COPD severity–associated metabolomic profiles of induced sputum. We also revealed the potential value of the induced sputum metabolomics for predicting the

severity of COPD. In addition, a subset of COPD severity-associated metabolites was identified, and the data indicate that the glycerophospholipid metabolism pathway plays a hub role in the progression of COPD and is thus likely a potential therapeutic target in COPD. Our results also suggest that the levels of SOD, MPO, and 8-iso-PGF 2α in induced sputum are potential biomarkers for predicting COPD severity. Collectively, our complex analysis of induced sputum at the metabolomics level not only provides confirmation of the association between the metabolomic profiles of induced sputum and COPD severity but also indicates the promising value of induced sputum metabolomics in the PPPM-based management of COPD. We hypothesized that induced sputum metabolites could be used to predict the progression, treatment response, and prognosis of COPD at an early stage, which would allow PPPM-based intervention in COPD.

We recommend the utilization of metabolomics in PPPM-associated studies of COPD. COPD is one of most common global diseases with high heterogeneity, and PPPM is a future trend for COPD management. Complicated metabolomic alterations are involved in different aspects of COPD. Metabolomics is a valuable and meaningful tool for the application of PPPM to COPD. Additionally, in future studies, the role of induced sputum metabolomics in the individual treatment response will be explored to further elucidate the value of metabolomics in the PPPM-based management of COPD. Specifically, based on individual metabolomic profiles, personalized management could be provided to patients with COPD.

Acknowledgments We want to express our sincere appreciation to all the patients who participated in the study. We would like to thank Shanghai Biotree Biotechnology for the LC-MS and data analyses.

Authors' contributions Zhihong Chen and Hong Ji conceived and designed the study. Shanqun Li, Lei Gao, Yuzhen Zeng, Ruolin Mao, Bo Cui, and Chunfang Liu collected the data. Tao Zhu, Shanqun Li, and Jijia Wang analyzed and interpreted the data. Tao Zhu, Zhihong Chen, and Jijia Wang drafted the manuscript. All authors read and approved the final manuscript.

Funding This study was supported by the National Natural Science Foundation of China (81470211 and 81970023), National Key Research and Development Program of China (No. 2018YFC1313600), the Shanghai Health Committee and Shanghai Respiratory Research Institute and Yang Scientists Training Program of Zhongshan Hospital (201840288), the Shanghai Top-Priority Clinical Key Disciplines Construction Project (2017ZZ02013), the Shanghai Municipal Key Clinical Specialty (shslczdzk02201), the Natural Science Foundation of Guangdong Province (2017A030310286), and the Scientific Research Project of Guangzhou (201707010282).

Compliance with ethical standards

Conflict of interest The authors declare that they have no conflict of interest.

Ethics approval This study was approved by the Research Ethics Committees of the Zhongshan Hospital of Fudan University (No. B2014-108) in accordance with the Declaration of Helsinki.

Consent for publication Not applicable.

Abbreviations 1-LGPC, 1-linoleoylglycerophosphocholine; ACO, asthma-COPD overlap; ALI, acute lung injury; COPD, chronic obstructive pulmonary disease; CRP, C-reactive protein; EPA, eicosapentaenoic acid; ESR, erythrocyte sedimentation rate; FEV1%, forced expiratory volume in 1st second %; FVC, forced vital capacity; GOLD, Global Initiative for Chronic Obstructive Lung Disease; GSH, glutathione; HRCT, high-resolution CT; ILDs, interstitial lung diseases; IQR, interquartile range; KEGG, Kyoto Encyclopedia of Genes and Genomes; LC-MS/MS, liquid chromatography-mass spectrometry; mMRC, Modified Medical Research Council Dyspnea Scale; MPO, myeloperoxidase; MS, mass spectrometry; MS1, mass spectrometry 1; MS2, mass spectrometry 2; NCE, normalized collision energy; NE, neutrophil elastase; NEG, negative; NMethy, *N*-methylethanolamine phosphate; OPLS-DA, orthogonal projections to latent structures discriminant analysis; PCA, principal component analysis; POS, positive; PTE, pulmonary thromboembolism; QC, quality control; RT, room temperature; SD, standard deviation; SHS, suboptimal health status; SOD, superoxide dismutase; TB, tuberculosis; VIP, variable importance in the projection

Open Access This article is licensed under a Creative Commons Attribution 4.0 International License, which permits use, sharing, adaptation, distribution and reproduction in any medium or format, as long as you give appropriate credit to the original author(s) and the source, provide a link to the Creative Commons licence, and indicate if changes were made. The images or other third party material in this article are included in the article's Creative Commons licence, unless indicated otherwise in a credit line to the material. If material is not included in the article's Creative Commons licence and your intended use is not permitted by statutory regulation or exceeds the permitted use, you will need to obtain permission directly from the copyright holder. To view a copy of this licence, visit <http://creativecommons.org/licenses/by/4.0/>.

References

- Adeloye D, Chua S, Lee C, Basquill C, Papana A, Theodoratou E, et al. Global and regional estimates of COPD prevalence: systematic review and meta-analysis. *J Glob Health*. 2015;5(2):020415. <https://doi.org/10.7189/jogh.05-020415>.
- GOLD. Global strategy for the diagnosis, management, and prevention of chronic obstructive pulmonary disease (Revised 2018). <https://goldcopd.org/> 2018.
- GBD 2013 Mortality and Causes of Death Collaborators. Global, regional, and national age-sex specific all-cause and cause-specific mortality for 240 causes of death, 1990–2013: a systematic analysis for the Global Burden of Disease Study 2013. *Lancet* 2015;385(9963):117–71. [https://doi.org/10.1016/s0140-6736\(14\)61682-2](https://doi.org/10.1016/s0140-6736(14)61682-2).
- Garudadi S, Woodruff PG. Targeting chronic obstructive pulmonary disease phenotypes, endotypes, and biomarkers. *Ann Am Thorac Soc*. 2018;15(Suppl 4):S234–s8. <https://doi.org/10.1513/AnnalsATS.201808-533MG>.
- Moon JY, Leitao Filho FS, Shahangian K, Takiguchi H, Sin DD. Blood and sputum protein biomarkers for chronic obstructive pulmonary disease (COPD). *Expert Rev Proteomics*. 2018;15(11):923–35. <https://doi.org/10.1080/14789450.2018.1539670>.






6. Wu HX, Zhuo KQ, Cheng DY. Peripheral blood eosinophil as a biomarker in outcomes of acute exacerbation of chronic obstructive pulmonary disease. *Int J Chron Obstruct Pulmon Dis*. 2019;14:3003–15. <https://doi.org/10.2147/copd.S226783>.
7. Tinè M, Biondini D, Semenzato U, Bazzan E, Cosio MG, Saetta M, et al. Reassessing the role of eosinophils as a biomarker in chronic obstructive pulmonary disease. *J Clin Med*. 2019;8(7). <https://doi.org/10.3390/jcm8070962>.
8. Barnes NC, Sharma R, Lettis S, Calverley PM. Blood eosinophils as a marker of response to inhaled corticosteroids in COPD. *Eur Respir J*. 2016;47(5):1374–82. <https://doi.org/10.1183/13993003.01370-2015>.
9. Franssen FM, Alter P, Bar N, Benedikter BJ, Iurato S, Maier D, et al. Personalized medicine for patients with COPD: where are we? *Int J Chron Obstruct Pulmon Dis*. 2019;14:1465–84. <https://doi.org/10.2147/copd.S175706>.
10. Sillen MJ, Franssen FM, Delbressine JM, Uszko-Lencer NH, Vanfleteren LE, Rutten EP, et al. Heterogeneity in clinical characteristics and co-morbidities in dyspneic individuals with COPD GOLD D: findings of the DICES trial. *Respir Med*. 2013;107(8):1186–94. <https://doi.org/10.1016/j.rmed.2013.04.020>.
11. Leung JM, Obeidat M, Sadatsafavi M, Sin DD. Introduction to precision medicine in COPD. *Eur Respir J*. 2019;53(4). <https://doi.org/10.1183/13993003.02460-2018>.
12. Ran N, Pang Z, Gu Y, Pan H, Zuo X, Guan X, et al. An updated overview of metabolomic profile changes in chronic obstructive pulmonary disease. *Metabolites*. 2019;9(6). <https://doi.org/10.3390/metabo9060111>.
13. Zhu Z, Camargo CA Jr, Hasegawa K. Metabolomics in the prevention and management of asthma. *Expert Rev Respir Med*. 2019;13(12):1135–8. <https://doi.org/10.1080/17476348.2019.1674650>.
14. Turi KN, Romick-Rosendale L, Ryckman KK, Hartert TV. A review of metabolomics approaches and their application in identifying causal pathways of childhood asthma. *J Allergy Clin Immunol*. 2018;141(4):1191–201. <https://doi.org/10.1016/j.jaci.2017.04.021>.
15. Wang H, Tian Q, Zhang J, Liu H, Zhang X, Cao W, et al. Population-based case-control study revealed metabolomic biomarkers of suboptimal health status in Chinese population-potential utility for innovative approach by predictive, preventive, and personalized medicine. *EPMA J*. 2020;11(2):147–60. <https://doi.org/10.1007/s13167-020-00200-7>.
16. Lu M, Zhan X. The crucial role of multiomic approach in cancer research and clinically relevant outcomes. *EPMA J*. 2018;9(1):77–102. <https://doi.org/10.1007/s13167-018-0128-8>.
17. Cheng T, Zhan X. Pattern recognition for predictive, preventive, and personalized medicine in cancer. *EPMA J*. 2017;8(1):51–60. <https://doi.org/10.1007/s13167-017-0083-9>.
18. Golubnitschaja O, Kinkorova J, Costigliola V. Predictive, preventive and personalised medicine as the hardcore of ‘Horizon 2020’: EPMA position paper. *EPMA J*. 2014;5(1):6. <https://doi.org/10.1186/1878-5085-5-6>.
19. Hu R, Wang X, Zhan X. Multi-parameter systematic strategies for predictive, preventive and personalised medicine in cancer. *EPMA J*. 2013;4(1):2. <https://doi.org/10.1186/1878-5085-4-2>.
20. Golubnitschaja O, Costigliola V. General report & recommendations in predictive, preventive and personalised medicine 2012: white paper of the European Association for Predictive, Preventive and Personalised Medicine *Epma j*. 2012;3(1):14. <https://doi.org/10.1186/1878-5085-3-14>.
21. Qian S, Golubnitschaja O, Zhan X. Chronic inflammation: key player and biomarker-set to predict and prevent cancer development and progression based on individualized patient profiles. *EPMA J*. 2019;10(4):365–81. <https://doi.org/10.1007/s13167-019-00194-x>.
22. Cruickshank-Quinn CI, Jacobson S, Hughes G, Powell RL, Petrache I, Kechris K, et al. Metabolomics and transcriptomics pathway approach reveals outcome-specific perturbations in COPD. *Sci Rep*. 2018;8(1):17132. <https://doi.org/10.1038/s41598-018-35372-w>.
23. Wang L, Tang Y, Liu S, Mao S, Ling Y, Liu D, et al. Metabonomic profiling of serum and urine by (1)H NMR-based spectroscopy discriminates patients with chronic obstructive pulmonary disease and healthy individuals. *PLoS One*. 2013;8(6):e65675. <https://doi.org/10.1371/journal.pone.0065675>.
24. Yu B, Flexeder C, McGarrah RW 3rd, Wyss A, Morrison AC, North KE, et al. Metabolomics identifies novel blood biomarkers of pulmonary function and COPD in the general population. *Metabolites*. 2019;9(4). <https://doi.org/10.3390/metabo9040061>.
25. Pinto-Plata V, Casanova C, Divo M, Tesfaigzi Y, Calhoun V, Sui J, et al. Plasma metabolomics and clinical predictors of survival differences in COPD patients. *Respir Res*. 2019;20(1):219. <https://doi.org/10.1186/s12931-019-1167-y>.
26. Fang W, Li C, Wu Q, Yao Z, Wu J, Huang P, et al. Metabolic profiling of chronic obstructive pulmonary disease model rats and the interventional effects of HuaTanJiangQi decoction using UHPLC-Q-TOF/MS(E). *J Pharm Biomed Anal*. 2020;180:113078. <https://doi.org/10.1016/j.jpba.2019.113078>.
27. Forton J. Induced sputum in young healthy children with cystic fibrosis. *Paediatr Respir Rev*. 2015;16(Suppl 1):6–8. <https://doi.org/10.1016/j.prrv.2015.07.007>.
28. Mussaffi H, Fireman EM, Mei-Zahav M, Prais D, Blau H. Induced sputum in the very young: a new key to infection and inflammation. *Chest*. 2008;133(1):176–82. <https://doi.org/10.1378/chest.07-2259>.
29. Chronic Obstructive Pulmonary Disease Committee. Respiratory Society CMA. [Guideline for diagnosis and treatment of chronic obstructive pulmonary disease (Version 2013)]. *Chin J Tuberc Respir Dis*. 2013;4(36):255–64.
30. David S, Edwards CW. Forced expiratory volume. *StatPearls*. Treasure Island (FL): StatPearls Publishing Copyright © 2020. Treasure Island: StatPearls Publishing LLC; 2020.
31. Lee TH, Jang AS, Park JS, Kim TH, Choi YS, Shin HR, et al. Elevation of S100 calcium binding protein A9 in sputum of neutrophilic inflammation in severe uncontrolled asthma. *Ann Allergy Asthma Immunol*. 2013;111(4):268–75.e1. <https://doi.org/10.1016/j.anai.2013.06.028>.
32. Boone JM, Hendee WR, McNitt-Gray MF, Seltzer SE. Radiation exposure from CT scans: how to close our knowledge gaps, monitor and safeguard exposure—proceedings and recommendations of the Radiation Dose Summit, sponsored by NIBIB, February 24–25, 2011. *Radiology*. 2012;265(2):544–54. <https://doi.org/10.1148/radiol.12112201>.
33. Kubo T, Ohno Y, Kauczor HU, Hatabu H. Radiation dose reduction in chest CT—review of available options. *Eur J Radiol*. 2014;83(10):1953–61. <https://doi.org/10.1016/j.ejrad.2014.06.033>.
34. Sellick CA, Hansen R, Stephens GM, Goodacre R, Dickson AJ. Metabolite extraction from suspension-cultured mammalian cells for global metabolite profiling. *Nat Protoc*. 2011;6(8):1241–9. <https://doi.org/10.1038/nprot.2011.366>.
35. Yang C, Du X, Hao R, Wang Q, Deng Y, Sun R. Effect of vitamin D3 on immunity and antioxidant capacity of pearl oyster *Pinctada fucata martensii* after transplantation: insights from LC-MS-based metabolomics analysis. *Fish Shellfish Immunol*. 2019;94:271–9. <https://doi.org/10.1016/j.fsi.2019.09.017>.
36. van der Does AM, Heijink M, Mayboroda OA, Persson LJ, Aanerud M, Bakke P, et al. Dynamic differences in dietary polyunsaturated fatty acid metabolism in sputum of COPD patients and controls. *Biochim Biophys Acta Mol Cell Biol Lipids*. 2019;1864(3):224–33. <https://doi.org/10.1016/j.bbalip.2018.11.012>.

37. Dunn WB, Broadhurst D, Begley P, Zelena E, Francis-McIntyre S, Anderson N, et al. Procedures for large-scale metabolic profiling of serum and plasma using gas chromatography and liquid chromatography coupled to mass spectrometry. *Nat Protoc.* 2011;6(7):1060–83. <https://doi.org/10.1038/nprot.2011.335>.
38. Bi J, Min Z, Yuan H, Jiang Z, Mao R, Zhu T, et al. PI3K inhibitor treatment ameliorates the glucocorticoid insensitivity of PBMCs in severe asthma. *Clin Transl Med.* 2020;9(1):22. <https://doi.org/10.1186/s40169-020-0262-5>.
39. Zhu T, Chen Z, Chen G, Wang D, Tang S, Deng H, et al. Curcumin attenuates asthmatic airway inflammation and mucus Hypersecretion involving a PPARgamma-dependent NF-kappaB signaling pathway in vivo and in vitro. *Mediat Inflamm.* 2019;2019:4927430–15. <https://doi.org/10.1155/2019/4927430>.
40. Zhu T, Li C, Zhang X, Ye C, Tang S, Zhang W, et al. GLP-1 analogue liraglutide enhances SP-A expression in LPS-induced acute lung injury through the TTF-1 signaling pathway. *Mediat Inflamm.* 2018;2018:3601454–14. <https://doi.org/10.1155/2018/3601454>.
41. Zhu T, Wu XL, Zhang W, Xiao M. Glucagon like peptide-1 (GLP-1) modulates OVA-induced airway inflammation and mucus secretion involving a protein kinase a (PKA)-dependent nuclear factor-kappaB (NF-kappaB) signaling pathway in mice. *Int J Mol Sci.* 2015;16(9):20195–211. <https://doi.org/10.3390/ijms160920195>.
42. Fortis S, Luszczek ER, Weinert CR, Beilman GJ. Metabolomics in COPD acute respiratory failure requiring noninvasive positive pressure ventilation. *Can Respir J.* 2017;2017:9480346–9. <https://doi.org/10.1155/2017/9480346>.
43. XueKe G, Shuai Z, JunYu L, LiMin L, LiJuan Z, JinJie C. Lipidomics and RNA-Seq study of lipid regulation in *Aphis gossypii* parasitized by *Lysiphlebia japonica*. *Sci Rep.* 2017;7(1):1364. <https://doi.org/10.1038/s41598-017-01546-1>.
44. Jing N, Liu X, Jin M, Yang X, Hu X, Li C, et al. Fubrick tea attenuates high-fat diet induced fat deposition and metabolic disorder by regulating gut microbiota and caffeine metabolism. *Food Funct.* 2020;11:6971–86. <https://doi.org/10.1039/d0fo01282c>.
45. Wu T, Yang L, Guo X, Zhang M, Liu R, Sui W. Raspberry anthocyanin consumption prevents diet-induced obesity by alleviating oxidative stress and modulating hepatic lipid metabolism. *Food Funct.* 2018;9(4):2112–20. <https://doi.org/10.1039/c7fo02061a>.
46. Dang VT, Zhong LH, Huang A, Deng A, Werstuck GH. Glycosphingolipids promote pro-atherogenic pathways in the pathogenesis of hyperglycemia-induced accelerated atherosclerosis. *Metabolomics.* 2018;14(7):92. <https://doi.org/10.1007/s11306-018-1392-2>.
47. Deng P, Barney J, Petriello MC, Morris AJ, Wahlang B, Hennig B. Hepatic metabolomics reveals that liver injury increases PCB 126-induced oxidative stress and metabolic dysfunction. *Chemosphere.* 2019;217:140–9. <https://doi.org/10.1016/j.chemosphere.2018.10.196>.
48. Wouters EF, Wouters BB, Augustin IM, Franssen FM. Personalized medicine and chronic obstructive pulmonary disease. *Curr Opin Pulm Med.* 2017;23(3):241–6. <https://doi.org/10.1097/mcp.0000000000000377>.
49. Reilly JJ. COPD and declining FEV1—time to divide and conquer? *N Engl J Med.* 2008;359(15):1616–8. <https://doi.org/10.1056/NEJMe0807387>.
50. Naz S, Kolmert J, Yang M, Reinke SN, Kamleh MA, Snowden S, et al. Metabolomics analysis identifies sex-associated metabolotypes of oxidative stress and the autotaxin-lysoPA axis in COPD. *Eur Respir J.* 2017;49(6). <https://doi.org/10.1183/13993003.02322-2016>.
51. Ghosh N, Choudhury P, Subramani E, Saha D, Sengupta S, Joshi M, et al. Metabolomic signatures of asthma-COPD overlap (ACO) are different from asthma and COPD. *Metabolomics.* 2019;15(6):87. <https://doi.org/10.1007/s11306-019-1552-z>.
52. Tan C, Huang H, Zhang J, He Z, Zhong X, Bai J. Effects of low-dose and long-term treatment with erythromycin on interleukin-17 and interleukin-23 in peripheral blood and induced sputum in patients with stable chronic obstructive pulmonary disease. *Mediat Inflamm.* 2016;2016:4173962–11. <https://doi.org/10.1155/2016/4173962>.
53. Gao J, Zhang M, Zhou L, Yang X, Wu H, Zhang J, et al. Correlation between fractional exhaled nitric oxide and sputum eosinophilia in exacerbations of COPD. *Int J Chron Obstruct Pulmon Dis.* 2017;12:1287–93. <https://doi.org/10.2147/copd.S134998>.
54. Gao J, Zhou W, Chen B, Lin W, Wu S, Wu F. Sputum cell count: biomarkers in the differentiation of asthma, COPD and asthma-COPD overlap. *Int J Chron Obstruct Pulmon Dis.* 2017;12:2703–10. <https://doi.org/10.2147/copd.S142466>.
55. Sol IS, Kim YH, Park YA, Lee KE, Hong JY, Kim MN, et al. Relationship between sputum clusterin levels and childhood asthma. *Clin Exp Allergy.* 2016;46(5):688–95. <https://doi.org/10.1111/cea.12686>.
56. Guiot J, Henket M, Corhay JL, Moermans C, Louis R. Sputum biomarkers in IPF: evidence for raised gene expression and protein level of IGFBP-2, IL-8 and MMP-7. *PLoS One.* 2017;12(2):e0171344. <https://doi.org/10.1371/journal.pone.0171344>.
57. Sobiecka M, Kus J, Demkow U, Filewska M, Jozwik A, Radwan-Rohrenscheff P, et al. Induced sputum in patients with interstitial lung disease: a non-invasive surrogate for certain parameters in bronchoalveolar lavage fluid. *J Physiol Pharmacol.* 2008;59(Suppl 6):645–57.
58. Xu C, Guo Z, Zhao C, Zhang X, Wang Z. Potential mechanism and drug candidates for sepsis-induced acute lung injury. *Exp Ther Med.* 2018;15(6):4689–96. <https://doi.org/10.3892/etm.2018.6001>.
59. Cao Z, Liu J, Xie X, Zhan S, Song W, Wu S, et al. Lipidomic profiling of amniotic fluid and its application in fetal lung maturity prediction. *J Clin Lab Anal.* 2019:e23109. <https://doi.org/10.1002/jcla.23109>.
60. Li F, Xiang B, Jin Y, Li C, Li J, Ren S, et al. Dysregulation of lipid metabolism induced by airway exposure to polycyclic aromatic hydrocarbons in C57BL/6 mice. *Environ Pollut.* 2019;245:986–93. <https://doi.org/10.1016/j.envpol.2018.11.049>.
61. Telenga ED, Hoffmann RF, Ruben TK, Hoonhorst SJ, Willemse BW, van Oosterhout AJ, et al. Untargeted lipidomic analysis in chronic obstructive pulmonary disease. Uncovering sphingolipids. *Am J Respir Crit Care Med.* 2014;190(2):155–64. <https://doi.org/10.1164/rccm.201312-2210OC>.
62. Kelly RS, Virkud Y, Giorgio R, Celedón JC, Weiss ST, Lasky-Su J. Metabolomic profiling of lung function in Costa Rican children with asthma. *Biochim Biophys Acta Mol basis Dis.* 2017;1863(6):1590–5. <https://doi.org/10.1016/j.bbadis.2017.02.006>.
63. Tabassum S, Haider S, Ahmad S, Madiha S, Parveen T. Chronic choline supplementation improves cognitive and motor performance via modulating oxidative and neurochemical status in rats. *Pharmacol Biochem Behav.* 2017;159:90–9. <https://doi.org/10.1016/j.pbb.2017.05.011>.
64. Sivanesan S, Taylor A, Zhang J, Bakovic M. Betaine and choline improve lipid homeostasis in obesity by participation in mitochondrial oxidative demethylation. *Front Nutr.* 2018;5:61. <https://doi.org/10.3389/fnut.2018.00061>.
65. Wang W, Ding XQ, Gu TT, Song L, Li JM, Xue QC, et al. Pterostilbene and allopurinol reduce fructose-induced podocyte oxidative stress and inflammation via microRNA-377. *Free Radic Biol Med.* 2015;83:214–26. <https://doi.org/10.1016/j.freeradbiomed.2015.02.029>.
66. de Bragança AC, RLM M, de Brito T, MHM S, Canale D, de Jesus DA, et al. Ecstasy induces reactive oxygen species, kidney water absorption and rhabdomyolysis in normal rats. Effect of N-

- acetylcysteine and Allopurinol in oxidative stress and muscle fiber damage. *PLoS One*. 2017;12(7):e0179199. <https://doi.org/10.1371/journal.pone.0179199>.
67. Xiong F, Li Q, Zhou B, Huang J, Liang G, Zhang L, et al. Oxidative stress and genotoxicity of long-term occupational exposure to low levels of BTEX in gas station workers. *Int J Environ Res Public Health*. 2016;13(12). <https://doi.org/10.3390/ijerph13121212>.
 68. Salimi A, Talatappe BS, Pourahmad J. Xylene induces oxidative stress and mitochondria damage in isolated human lymphocytes. *Toxicol Res*. 2017;33(3):233–8. <https://doi.org/10.5487/tr.2017.33.3.233>.
 69. Zhao T, Zhang H, Zhao T, Zhang X, Lu J, Yin T, et al. Intrarenal metabolomics reveals the association of local organic toxins with the progression of diabetic kidney disease. *J Pharm Biomed Anal*. 2012;60:32–43. <https://doi.org/10.1016/j.jpba.2011.11.010>.
 70. Wang YX, Wu Y, Chen HG, Duan P, Wang L, Shen HQ, et al. Seminal plasma metabolome in relation to semen quality and urinary phthalate metabolites among Chinese adult men. *Environ Int*. 2019;129:354–63. <https://doi.org/10.1016/j.envint.2019.05.043>.
 71. Liu J, Xiao HT, Wang HS, Mu HX, Zhao L, Du J, et al. Halofuginone reduces the inflammatory responses of DSS-induced colitis through metabolic reprogramming. *Mol Biosyst*. 2016;12(7):2296–303. <https://doi.org/10.1039/c6mb00154h>.
 72. Lu H, Ding J, Liu W, Peng Z, Chen W, Sun X, et al. UPLC/MS-based metabolomics investigation of the protective effect of hydrogen gas inhalation on mice with calcium oxalate-induced renal injury. *Biol Pharm Bull*. 2018;41(11):1652–8. <https://doi.org/10.1248/bpb.b18-00307>.
 73. Wang P, Wang HP, Xu MY, Liang YJ, Sun YJ, Yang L, et al. Combined subchronic toxicity of dichlorvos with malathion or pirimicarb in mice liver and serum: a metabonomic study. *Food Chem Toxicol*. 2014;70:222–30. <https://doi.org/10.1016/j.fct.2014.05.027>.
 74. Lukowicz C, Ellero-Simatos S, Régnier M, Polizzi A, Lasserre F, Montagner A, et al. Metabolic effects of a chronic dietary exposure to a low-dose pesticide cocktail in mice: sexual dimorphism and role of the constitutive androstane receptor. *Environ Health Perspect*. 2018;126(6):067007. <https://doi.org/10.1289/ehp2877>.
 75. Ahmad A, Herndon DN, Szabo C. Oxandrolone protects against the development of multiorgan failure, modulates the systemic inflammatory response and promotes wound healing during burn injury. *Burns*. 2019;45(3):671–81. <https://doi.org/10.1016/j.burns.2018.10.006>.
 76. Herndon DN, Voigt CD, Capek KD, Wurzer P, Guillory A, Kline A, et al. Reversal of growth arrest with the combined administration of oxandrolone and propranolol in severely burned children. *Ann Surg*. 2016;264(3):421–8. <https://doi.org/10.1097/sla.0000000000001844>.
 77. Li Z, Yang L, Liu Y, Xu H, Wang S, Liu Y, et al. Anti-inflammatory and antioxidative effects of Dan-Lou tablets in the treatment of coronary heart disease revealed by metabolomics integrated with molecular mechanism studies. *J Ethnopharmacol*. 2019;240:111911. <https://doi.org/10.1016/j.jep.2019.111911>.

Publisher's note Springer Nature remains neutral with regard to jurisdictional claims in published maps and institutional affiliations.

Affiliations

Tao Zhu¹  · Shanqun Li²  · Jiajia Wang³  · Chunfang Liu² · Lei Gao² · Yuzhen Zeng² · Ruolin Mao²  · Bo Cui² · Hong Ji⁴  · Zhihong Chen² 

¹ Respiratory Medicine, Second Affiliated Hospital of Chongqing Medical University, Chongqing 400010, China

² Department of Respiratory and Critical Care Medicine, Zhongshan Hospital of Fudan University, Shanghai 20032, China

³ Rheumatology Medicine, Second Affiliated Hospital of Chongqing Medical University, Chongqing 400010, China

⁴ California National Primate Research Center, and Department of Anatomy, Physiology & Cell Biology, School of Veterinary Medicine, University of California, Davis, CA 95616, USA